PHYSICAL REVIEW B **67**, 020404(R) (2003)

Transition from Curie-Weiss to enhanced Pauli paramagnetism in $R\mathrm{NiO_3}$ (R=La,Pr,…Gd)

J.-S. Zhou,[1] J. B. Goodenough,[1] and B. Dabrowski[2]
[1]*Texas Materials Institute, University of Texas at Austin, ETC 9.102, Austin, Texas 78712*
[2]*Physics Department, Northern Illinois University, FW 216, DeKalb, Illinois 60115*
(Received 11 November 2002; published 22 January 2003)

High-oxygen-pressure annealing, cold pressing, and measurement of properties under pressure have been used to reveal and to follow in the single-valent perovskites $R\mathrm{NiO_3}$ (R=lanthanide) a crossover from localized to itinerant electronic behavior. Cold pressing proved critical for obtaining nearly intrinsic transport properties such as electronic and thermal conductivity in polycrystalline samples not available as single crystals. Suppression of the thermal conductivity in the crossover compositions $\mathrm{NdNiO_3}$ and $\mathrm{PrNiO_3}$ suggests cooperative bond-length fluctuations in this region.

DOI: 10.1103/PhysRevB.67.020404 PACS number(s): 66.70.+f, 71.70.Gm, 75.30.Et

The evolution of the physical properties at the crossover from localized to itinerant electronic behavior in the transition-metal perovskite-related oxides remains a fundamental problem of solid-state physics. High-T_c superconductivity in the cuprates and a colossal magnetoresistance in the manganites are examples of the unusual properties that are found in mixed-valent compounds at this crossover. The $R\mathrm{NiO_3}$ (R=lanthanide) perovskites provide an opportunity to study this crossover in a series of single-valent compounds where the transition occurs among electrons in σ-bonding orbitals and the π-bonding orbitals are filled.

$\mathrm{LaNiO_3}$ is metallic with an enhanced Pauli paramagnetism,[1] and reducing the size of the lanthanide ion narrows the width of the σ^* conduction band so as to allow entering the transition region from the itinerant-electron side. The compounds with Y and R=Sm to Lu are Curie-Weiss paramagnetic insulators below a first-order insulator-metal transition temperature T_{IM} with a Néel temperature T_N ($<T_{\mathrm{IM}}$) that increases progressively with the equilibrium (R-O) bond length and hence with the tolerance factor $t \equiv (R\text{-O})/\sqrt{2}(\text{Ni-O})$ (Fig. 1). This situation allows approaching the crossover from the localized-electron side also. In the crossover compositions with $R=\mathrm{Sm_{1-x}Nd_x}$ to $\mathrm{Pr_{1-x}La_x}$, T_N is defined by the first-order transition at T_{IM}, which decreases with increasing t; this observation led to the suggestion that a Mott-Hubbard transition is occurring at T_{IM}.[2]

However, the structure below T_{IM} is distorted from orthorhombic *Pbnm* to monoclinic $P2_1/n$ in which the nearly simple-cubic array of Ni atoms is split into two interpenetrating face-centered-cubic arrays with distinguishable Ni_I and Ni_{II} atoms;[3–5] the lower symmetry provides an additional mechanism for splitting of the narrow σ^* band below T_{IM}. TEM, Raman scattering, and x-ray absorption spectroscopy have provided more precise structural information that shows the structural change to $P2_1/n$ symmetry below T_{IM} extends to $\mathrm{NdNiO_3}$,[6,7] but the monoclinic distortion is small. From the valence-bond sum model, a charge disproportionation in the $\mathrm{NiO_3}$ array was deduced for the $R\mathrm{NiO_3}$ (R=Ho,Y,…,Lu).[3–5] Efforts have been given to understand the unusual spin ordering found below T_N.[8–10] On the other hand, samples with $T_N<T_{\mathrm{IM}}$ exhibit a $T_N \sim \cos^2\theta$, where θ is the Ni—O—Ni bond angle;[11,12] this bond-angle dependence is characteristic of superexchange interactions between localized d-electron configurations, but it may not be compatible with disproportionation in the $\mathrm{NiO_3}$ array. Localized t^6e^1 configurations can be expected to introduce cooperative Jahn-Teller distortions that could have different character at Ni_I and Ni_{II} atoms. Rodriguez-Carvajal *et al.*[9] have rationalized the unusual spin ordering below T_N with different cooperative Jahn-Teller distortions at the Ni_I and Ni_{II} atoms.

Only a small change in tolerance factor from $t \approx 0.968$ to 0.985 separates $\mathrm{SmNiO_3}$ and the composition where T_{IM} falls to zero, yet there is a change from Curie-Weiss to enhanced Pauli paramagnetism across this interval. In this paper we probe how several physical properties change across this interval; and, by tuning the σ^* bandwidth with hydrostatic pressure, we demonstrate that $\mathrm{SmNiO_3}$ is located at the threshold where the localized-electron superexchange model fails. Measurements of the thermal conductivity have demonstrated that phonons are strongly suppressed in the compositions $\mathrm{NdNiO_3}$ and $\mathrm{PrNiO_3}$ of the crossover compositions.

The materials used in this work were synthesized under a high oxygen pressure at the Northern Illinois University (NIU) as in previous studies.[13,14] As made, the samples are

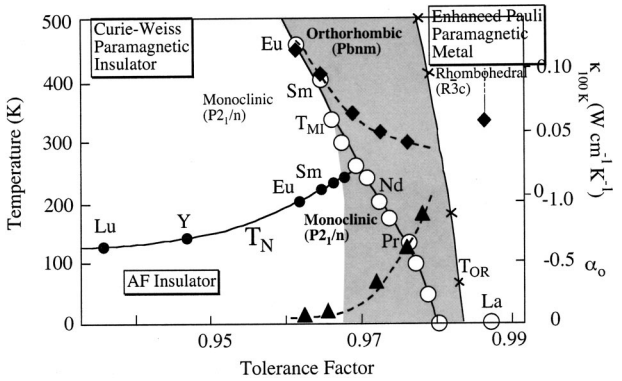

FIG. 1. Schematic phase diagram of the $R\mathrm{NiO_3}$ (R=La...Lu) family. The shaded area is the two-phase region (see the text). The triangle symbol is for the oxygen isotope effect on T_{IM} (see the text), the diamond is for the lattice contribution of the thermal conductivity at 100 K. The circles are from Ref. 1, and T_{OR} is from Ref. 11.

 ©2003 The American Physical Society

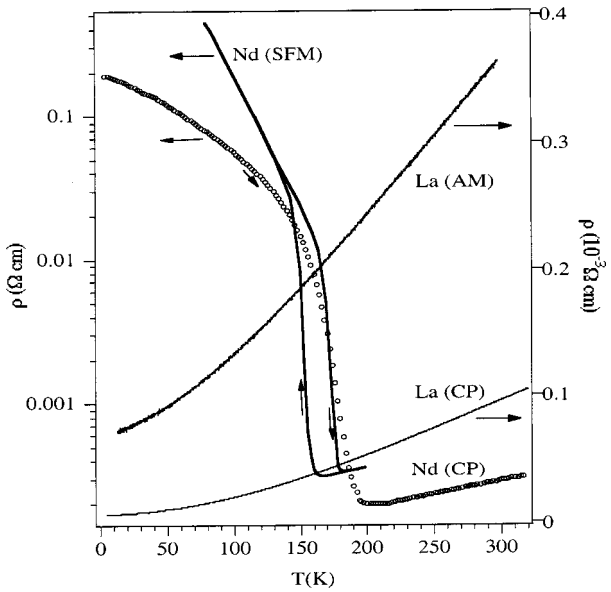

FIG. 2. Temperature dependence of the resistivity in the $LaNiO_3$ and $NdNiO_3$ samples. SFM denotes a single crystal film; AM: as made samples; and CP: a cold-pressed sample.

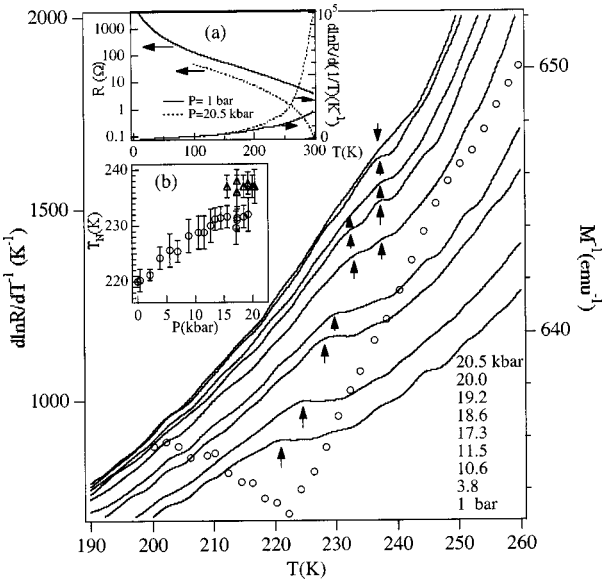

FIG. 3. Typical temperature dependence of the derivative $d\ln R/dT^{-1}$ and the reverse magnetization of the cold-pressed $SmNiO_3$ under pressure. The pressures labeled in the lower right corner correspond to the curves in the order from the top. For the same sample, inset (a) is the temperature dependence of the resistance under pressure, and inset (b) is the pressure dependence of T_N.

highly porous and soft. In order to preserve the high chemical quality while obtaining fully dense samples, a cold-pressing procedure was developed at the University of Texas at Austin (UTA). In this procedure, $R NiO_3$ powders were reground and pressed into pellets. The pellets were then placed in a 3-mm-diameter hole drilled in the center of a gasket made of a dense, strong cardboard and loaded between two tungsten-carbide (WC) anvils. The gasket was subjected to an average pressure of 10 kbar, but on the sample at the gasket center pressures might have reached as high as 100 kbar as judged by viewing, after release of pressure, a shallow dent made at the surface of the WC anvils. The surface of a thin cold-pressed sample has a metallic shine and is harder than heat-treated carbon steel. These bars were annealed at 1100 °C under 600-bar oxygen for 24 h at the NIU in order to let the grains grow. Samples that had undergone this procedure had the identical transition temperatures T_N and T_{IM} obtained for the as-made samples shown in Fig. 1, but the transport properties were dramatically improved. As shown in Fig. 2, the cold-pressed (CP) $\times(LaNiO_3)$ resistivity was three times lower than that of the as-made $LaNiO_3$. In fact, $\rho(T)$ for CP $LaNiO_3$ is as low or lower than most single-crystal metallic oxides; the CP $NdNiO_3$ $\rho(T)$ reaches the same level obtained with single-crystal $NdNiO_3$ films.[7] The availability of high-density samples allowed us to investigate the thermal conductivity and to compare it with that obtained on single-crystal Fe_3O_4, a conductive spinel undergoing charge ordering at the Verwey temperature $T_V \approx 122$ K. The Fe_3O_4 crystal was grown at the UTA in an infrared-heating image furnace under an argon atmosphere. Laue back diffraction and the sharp first-order transition at T_V from the specific heat showed an Fe_3O_4 crystal of superb quality with nearly perfect chemical stoichiometry. Measurements of $\rho(T)$ under pressure were performed in a Be-Cu self-clamped cell; a steady-state method was used to obtain the thermal conductivity $\kappa(T)$.[15]

In order to monitor how T_N varies with the bandwidth as the crossover is approached from the localized-electron side, we chose to measure the resistance $R(T)$ of $SmNiO_3$ as a function of pressure; as in other antiferromagnetic insulators such as $LaTiO_3$ (Ref. 16) and $Ca_{1-x}Sr_xMnO_3$,[17] $d\ln R/d(1/T)$ shows an anomaly at T_N; see inset (a) of Fig. 3, where $R(T)$ changes smoothly. The correspondence of this anomaly with T_N is shown in Fig. 3 at 1 bar; the figure also shows the evolution of the anomaly with pressure and, in inset (b), the corresponding linear increase in T_N with pressure to $P=15$ kbar; at higher pressures, the appearance of two pressure-independent anomalies, though not as clear as the transition at T_N in low-pressure range, signals the presence of two phases each with a somewhat different T_N. At $P=20.5$ kbar, the highest pressure of this work, T_{IM} is lowered from 400 K at ambient pressure to near room temperature, but a $T_N < T_{IM}$ is retained. The Bloch coefficient $\alpha_B \equiv (T_N^{-1} dT_N/dP)/(V^{-1}dV/dP)$ has been found empirically[18] and justified theoretically for a constant on-site correlation energy U to have a value $\alpha_B \approx 3.3$. Linear fitting of the data of Fig. 3 in the range $P \leqslant 15$ kbar gives a $T_N^{-1} dT_N/dP = 3.6\times10^{-3}$ $(\text{kbar})^{-1}$, and high-pressure neutron diffraction data[19] for $PrNiO_3$ gives a compressibility $V^{-1}dV/dP = 0.656\times10^{-3}$ $(\text{kbar})^{-1}$. Given that the compressibility of $SmNiO_3$ is the same as that of $PrNiO_3$, the resulting $\alpha_B = 5.5 > 3.3$ implies that the assumption of a constant on-site energy U or charge-transfer gap Δ is not valid in $SmNiO_3$ and that $SmNiO_3$ is therefore at the threshold where the localized-electron superexchange model breaks down. A similar observation[20] has been made on $LaMnO_3$

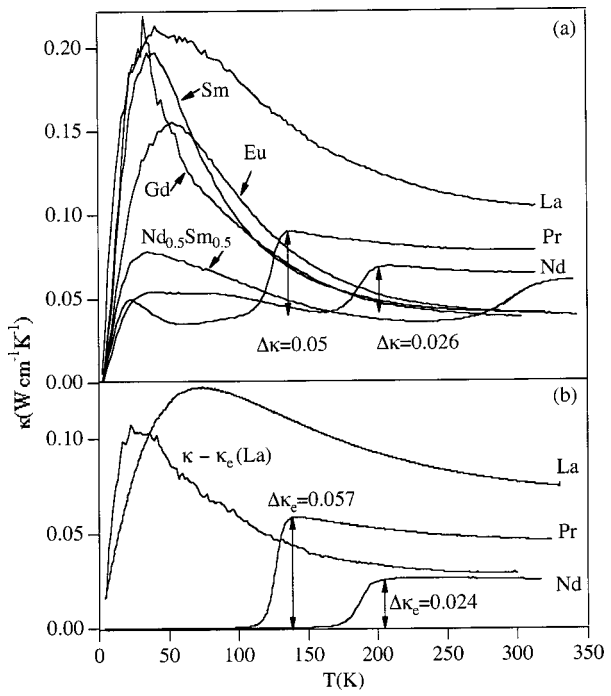

FIG. 4. (a) Temperature dependence of the thermal conductivity in the cold-pressed samples $R\mathrm{NiO_3}$ (the R is labeled on each curve) (b) The upper-bound electronic contribution to the thermal conductivity in cold-pressed $R\mathrm{NiO_3}$ (R=La, Pr, and Nd) calculated from the resistivity in the corresponding samples via the Wiedemann-Franz law.

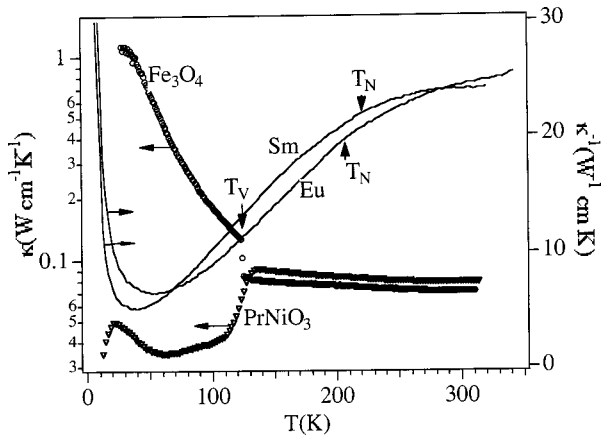

FIG. 5. Temperature dependence of the thermal conductivity in single-crystal Fe_3O_4, together with the CP $PrNiO_3$ and inverse thermal conductivity of cold-pressed $SmNiO_3$ and $EuNiO_3$. The Verwey transition temperature T_V is shown on the Fe_3O_4 curve.

where the existence of a small charge-transfer gap Δ has been proven experimentally.[21] The two-phase region found for $P>15$ kbar is like that found for $LaMnO_3$ and supports our contention that two-phase fluctuations are a characteristic feature of crossover compositions. We have shown in other systems[15] that the two-phase fluctuations suppress the phonon contribution to the thermal conductivity. Therefore, we turn to measurement of the thermal conductivity $\kappa(T)$ of the $R\mathrm{NiO_3}$ compounds.

Figure 4(a) shows the $\kappa(T)=\kappa_e(T)+\kappa_{\mathrm{latt}}(T)$ obtained for samples with different R. The electronic contribution $\kappa_e(T)$ makes $\kappa(T)$ for the metallic temperature range of R = La, Pr, Nd, and $Nd_{0.5}Sm_{0.5}$ higher than the $\kappa(T)=\kappa_{\mathrm{latt}}$ of the insulators R=Sm, Eu, Gd at room temperature. In order to obtain the lattice contribution κ_{latt} in the metallic temperature range, we use the Wiedemann-Franz law to calculate from our measured $\rho(T)$ the *upper bound* of the electronic contribution κ_e shown in Fig. 4(b). $\kappa_{\mathrm{latt}}=\kappa-\kappa_e$ for $LaNiO_3$, which is a *lower bound* for the lattice contribution, remains phononlike as for the insulators R=Sm, Eu, Gd. Samples R=Pr, Nd, $Nd_{0.5}Sm_{0.5}$ show a κ_e that vanishes abruptly at T_{IM}; the calculated $\Delta\kappa_e$ at T_{IM} matches well the $\Delta\kappa$ of Fig. 4(a) occurring at T_{IM}. Since $\Delta\kappa_e$ is an upper bound of the electronic contribution, we conclude that the lattice contribution also drops on cooling through T_{IM}; it certainly does not increase as shown in Fig. 5 for Fe_3O_4 on cooling through its insulator-conductive transition at T_V. Moreover, the identical temperature dependence of κ and κ_e in the metallic range for R=Pr, Nd, $Nd_{0.5}Sm_{0.5}$ shows that κ_{latt} has little temperature dependence in the metallic range of these samples. More striking is the $d\kappa_{\mathrm{latt}}/dT>0$ below $T_{\mathrm{IM}}=T_N$ in $PrNiO_3$, which is opposite to the normal $d\kappa_{\mathrm{latt}}/dT<0$ found for the metallic phase R=La, and the insulator phases R=Sm, Eu, and Gd. A phonon contribution in κ_{latt} appears to be partially restored in the $R=Nd_{0.5}Sm_{0.5}$ sample below T_{IM}.

A sharp difference can be seen in Fig. 5 between $\kappa_{\mathrm{latt}}(T)$ below T_{IM} in R=Pr, Nd and that below $T_V=Fe_3O_4$ where a complex charge ordering of polarons occurs.[22] This difference highlights the new physics that is encountered at the crossover from localized to itinerant electronic behavior. Suppression of κ_{latt} below $T_N=T_{\mathrm{IM}}$ in $PrNiO_3$ and $NdNiO_3$ shows that the spin ordering does not restore the phonon structure of the lattice; this situation may occur where there are two-phase fluctuations. Without speculation on how the bond lengths fluctuate below $T_N=T_{\mathrm{IM}}$, we can state unambiguously that *phonons are suppressed in compounds at the crossover from Curie-Weiss to Pauli paramagnetism*. Independent photoemission data[23] support the presence of two-phase fluctuations in $PrNiO_3$ and $NdNiO_3$; they show a continuous transfer of spectral weight from the Fermi energy with decreasing $T<T_{\mathrm{IM}}$, which shows the metallic phase does not disappear abruptly as the strong-correlation fluctuations order into a percolating phase below $T_N=T_{\mathrm{IM}}$. Moreover, a large oxygen-isotope coefficient $\alpha_o\equiv -d\ln T_{\mathrm{IM}}/d\ln M$,[24] shown together with κ_{latt}(100 K) in Fig. 1, demonstrates that oxygen vibrations play an essential role not only in T_{IM}, but also in the suppression of κ_{latt}, and that this role increases dramatically as the tolerance factor t increases to where T_{IM} falls to zero on the approach to the orthorhombic-rhombohedral phase transition T_{OR}. The oxygen vibrations modulate (Ni—O) bond-length fluctuations that may occur not only at fluctuating phase boundaries, but also at dynamic Jahn-Teller deformations associated with localized-electron e^1 configurations. Since the volume fraction of the antiferromagnetic phase can be presumed to reach percolation below T_{IM}, suppression of $\kappa(T)$ below T_{IM} suggests that any local Jahn-Teller deformation in the phase fluctuate. Another example of this behavior has been found

in the mixed-valent system $La_{1-x}Sr_xMnO_3$ at the crossover from localized to itinerant electronic behavior,[14] but in this case the *e*-electron spin is coupled strongly to a spin $S=\frac{3}{2}$ from half-filled t^3 orbitals whereas $LaNiO_3$ has a filled t^6 configuration.

Figure 5 also displays $1/\kappa_{\rm latt}(T)$ for $R=$ Sm, Eu; the curves shows a clear deviation from the $1/T$ law at $T>T_N$. As discussed elsewhere for other antiferromagnetic insulators,[25] this suppression is due to a strong spin-lattice interaction found for insulators with a charge-transfer gap Δ. The local (Ni—O) bond-length fluctuations due to the spin fluctuations are reduced at temperatures $T<T_N$. A more severe deviation from a $1/T$ law in $SmNiO_3$ compared to $EuNiO_3$ is consistent with a smaller U and Δ in $SmNiO_3$ due to its approach to the crossover condition.

In conclusion, the relation $T_N\sim\cos^2\theta$ in $RNiO_3$ ($R=$ Sm-Lu) and the coefficient $dT_N/dP>0$ found in $SmNiO_3$ confirms that the *e* electrons at the low-spin Ni(III):t^6e^1 ions of $RNiO_3$ are localized in the monoclinic $P2_1/n$ insulator phase where Curie-Weiss paramagnetism is found in an interval $T_N<T<T_{\rm IM}$. However, a Bloch coefficient $\alpha_B=5.5>3.3$ locates $SmNiO_3$ at the threshold of a crossover to the itinerant-electron behavior found in rhombohedral $LaNiO_3$. $NdNiO_3$ and $PrNiO_3$ fall in the crossover region; they have a $T_N=T_{\rm IM}$ and a suppressed $\kappa_{\rm latt}$ in both the metallic and magnetic-insulator phases. Suppression of $\kappa_{\rm latt}$ is correlated with a giant isotope effect on $T_{\rm IM}$, which demonstrates that fluctuating oxygen displacements that modulate (Ni—O) bond lengths are responsible for suppression of $\kappa_{\rm latt}$ as well as for the isotope effect. The fluctuating oxygen displacements are thought to be cooperative, defining fluctuating localized and itinerant electronic phases as well as responding to fluctuating Jahn-Teller and/or disproportionation deformations within the localized-electron phase. The localized-electron phase and the metallic phase fluctuate in the range $T_{\rm IM}<T<T_{\rm OR}$. The volume fraction of the localized-electron phase increases discontinuously on cooling through the first-order transition at $T_{\rm IM}$.

We acknowledge the financial support of the NSF [DMR0132282 (J.B.G.), DMR0105398 (B.D.)], the TCSUH of Houston, TX (J.B.G.), and the Robert A. Welch Foundation of Houston, TX (J.B.G.).

[1] J. B. Goodenough and P. Raccah, J. Appl. Phys. **36**, 1031 (1965).
[2] J. B. Torrance *et al.*, Phys. Rev. B **45**, 8209 (1992).
[3] J. A. Alonso *et al.*, Phys. Rev. Lett. **82**, 3871 (1999).
[4] J. A. Alonso *et al.*, Phys. Rev. B **61**, 1756 (2000).
[5] J. A. Alonso *et al.*, Phys. Rev. B **64**, 094102 (2001).
[6] M. Zaghrioui *et al.*, Phys. Rev. B **64**, 081102 (2001).
[7] U. Staub *et al.*, Phys. Rev. Lett. **88**, 126402 (2002).
[8] J. L. Garcia-Munoz *et al.*, Phys. Rev. B **50**, 978 (1994).
[9] J. Rodriguez-Crvajal *et al.*, Phys. Rev. B **57**, 456 (1998).
[10] M. T. Fernandez-Diaz *et al.*, Phys. Rev. B **64**, 144417 (2001).
[11] M. L. Medarde, J. Phys.: Condens. Matter **9**, 1679 (1997).
[12] J. A. Alonso *et al.*, Phys. Rev. B **61**, 1756 (2000).
[13] J.-S. Zhou *et al.*, Phys. Rev. Lett. **84**, 526 (2000).
[14] J.-S. Zhou, J. B. Goodenough, and B. Dabrowski, Phys. Rev. B **61**, 4401 (2000).
[15] J.-S. Zhou and J. B. Goodenough, Phys. Rev. B **64**, 024421 (2001).
[16] Y. Okada *et al.*, Phys. Rev. B **48**, 9677 (1993).
[17] O. Chmaissem *et al.*, Phys. Rev. B **64**, 134412 (2001).
[18] D. Bloch, J. Phys. Chem. Solids **27**, 881 (1966).
[19] M. Medarde *et al.*, Phys. Rev. B **52**, 9248 (1995).
[20] J.-S. Zhou and J. B. Goodenough, Phys. Rev. Lett. **89**, 087201 (2002).
[21] J.-S. Zhou and J. B. Goodenough, Phys. Rev. B **60**, R15 002 (1999).
[22] J. P. Wright, J. P. Attfield, and P. G. Radaelli, Phys. Rev. Lett. **87**, 266401 (2001).
[23] I. Vobornik *et al.*, Phys. Rev. B **60**, R8426 (1999).
[24] M. Medarde *et al.*, Phys. Rev. Lett. **80**, 2397 (1998).
[25] J.-S. Zhou and J. B. Goodenough, Phys. Rev. B **66**, 052401 (2002).